Failure analysis of electrical-thermal-optical characteristics of LEDs based on AlGaInP and InGaN/GaN

© Huanting Chen [*], Arno Keppens [◊], Peter Hanselaer [◊], Yijun Lu [+¶], Yulin Gao [+], Rongrong Zhuang [*], Zhong Chen [+¶]

[*] Department of Physics & Electronic Information Engineering, Zhangzhou Normal University, Zhangzhou, Fujian, 363000 P. R. China
[+] Department of Electronic Science, Fujian Engineering Research Center for Solid-State Lighting, Xiamen University, Xiamen, Fujian, 361005 P. R. China
[◊] Light & Lighting Laboratory, Catholic University College Gent, Gebroeders De Smetstraat 1, B-9000 Gent, Belgium

(Получена 20 марта 2012 г. Принята к печати 25 марта 2012 г.)

The electrical-thermal-optical characteristics of AlGaInP yellow and InGaN/GaN blue LEDs under electrical stresses were studied. Since the increase of effective acceptor concentration on p-type side, the forward voltages of AlGaInP decrease after 3155 h aging. And the operating voltage of high forward bias expansion for InGaN/GaN is due to the increase of the series resistance. Compared with InGaN/GaN, AlGaInP LEDs display different trend for the relationship between optical output and ideality factors. The relationship between ideality factor and radiative recombination is also studied and established. The characteristic of different intermediate adhesive is compared during aging period based on transient thermal test.

1. Introduction

Recent applications of LEDs, such as general lighting and television backlighting, require an extended long-term stability. The reliability of LEDs has a close contact with degradation mechanism. The main degradation mechanism factors include dark spot defects [1], contact metal migration [2], composition fluctuation [3], solder instability, recombination-enhanced defect formation and thermally induced defect formation [4], negative capacitance-conductance effect [5] etc. This degradation speed is enhanced by electrical-thermal stresses. The properties of LED can be evaluated by ideality factor, extracted from the current-voltage characteristic. Thermal resistance is an important factor for evaluating the reliability of LED. Adhesive layer contributes to major thermal resistance for LED package. The materials of intermediate adhesive layers for die attachment are silver epoxy and insulative adhesive in LED manufactures. High thermal-electrical stresses will increase contact thermal resistance so as to lead to LED failure [6,7]. A. Uddin et al studied the degradation mechanism of GaN-based blue LED by the current-voltage and light-current characteristics under 20, 40 and 60 mA, respectively [8]. M. Meneghini et al studied the degradation processes at temperatures ranging from 180 to 230°C [9]. There are, however, only a few reports on the LEDs degradation combining optical output, ideality factor with thermal characteristics study together. In this paper, based on current-voltage curve, optical output and thermal resistance measurements, AlGaInP and InGaN/GaN LEDs aging test were conducted under different electrical stresses, and the failure mechanism was studied and discussed. During aging process, the ideality factor is highly related to the LED optical output. The ideality factors of different electrical stresses and the thermal resistance based on intermediate adhesive layer are compared and discussed during aging test.

¶ E-mail: yjlu@xmu.edu.cn
chenz@xmu.edu.cn

2. Experiment

This study explored the degradation of LED's optical output, current-voltage characteristic properties and thermal resistance as a function of time under electrical stresses of 20, 40, 60 and 80 mA, respectively, at ambient temperature of 25°C. The optical output and current-voltage curve of the LED were measured. The thermal resistance was measured by transient thermal tester (T3ster) and Teraled system. Transient thermal measurement was done in the following procedures. The first step was to calibrate the temperature-voltage sensitive parameter of LED. The temperature-voltage sensitive parameter (TSP factor) was done based on Eq. (1). The calibration process was measured with the temperature ranged from 25 to 55°C and 1 mA sensing current for LEDs with avoiding self-heating effect.

$$TSP = \Delta T_J/\Delta V_F, \tag{1}$$

Where ΔT_J is the response junction temperature of LED, ΔV_F is the variation of forward voltage. And then after driving the current of 20 mA for 20 min at the ambient temperature of 25° to reach the thermal stabilization, the cooling curve was started to capture. T3ster captured the real time thermal transient response of the forward voltage of LED, then derived the thermal characteristics by evaluating the thermal transient response curve based on the structure function. The theoretical framework of evaluation of T3ster was based on the RC distribution

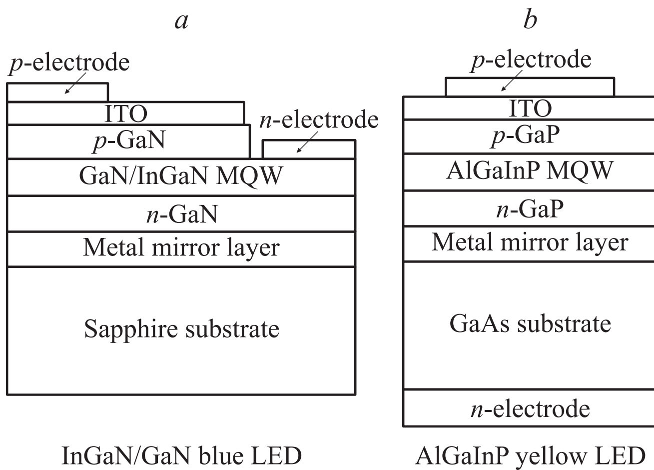

Figure 1. The chip structures of AlGaInP and InGaN/GaN LED.

networks [10–12]. So that the thermal resistance of different material could be determined quantitatively from cumulative structure function. This function plotted the C_Σ cumulative capacitance as the function of the R_Σ cumulative resistance of the heat flow path within the samples

$$C_\Sigma = \int_0^x c(\xi)A(\xi)d\xi, \quad (2)$$

$$R_\Sigma = \int_0^x \frac{d\xi}{\lambda(\xi)A(\xi)}, \quad (3)$$

where c is the volumetric heat capacitance, λ is the thermal conductivity, $A(x)$ is the cross-sectional area of the heat flow path. The $x = 0$ basis is usually the junction node of LED.

Fig. 1 shows the chip structures of AlGaInP and InGaN/GaN LED. It is noted that indium tin oxide (ITO) is used as a current spreading layer. ITO is expected to provide a more uniform current spreading in an LED die, since it has the electric conductivity much greater than that of the p-GaN contact layer. Multiple quantum well structure (MQW) is formed by laminating at least two pairs of quantum well layers each having a thickness substantially equal to the de-Broglie's wave-length of electrons and barrier layers of an energy gap greater than that of the quantum well layers. Samples applied under different electrical stress currents: 20, 40, 60 and 80 mA, in a thermally controlled oven with ambient temperature of 25°C.

3. Result and discussion

Fig. 2 shows $I-V$ characteristics of AlGaInP yellow and InGaN/GaN blue LEDs as a function of stress time under electrical stress of 20 mA. It is found that the forward voltage of InGaN/GaN blue LED increases from 3.271 to 3.562 V after 3155 h at measured current of 80 mA, respectively. However, it is noted that after aging 3155 h, the forward voltage (driven with 80 mA) of AlGaInP yellow LED decrease from 2.115 to 2.062 V, respectively. Because the electrical characteristics of the LED are related to the Mg–H bonds and active acceptor concentration. The reduction of the active acceptor concentration, due to the interaction between hydrogen and magnesium, can worsen the properties of anode contact, induce the degradation of the ohmic contact at the p-side [13]. Therefore, the forward voltages of yellow LEDs descend as stress time increase with overall trend, which is due to an increase in the effective acceptor concentration on p-type side. During aging process, electrons can disrupt residual complexes Mg–H on the border of the active layer in p-GaN and p-GaP. Thus, the hydrogen goes out of complexes and the charge of Mg-ions will be compensated by holes. The existing high density threading dislocations from the large differences in the lattice-mismatch and thermal-expansion coefficient between GaN epilayer and sapphire substrate have also great influence on LED's forward voltage [14,15]. The contact metals may electromigrate along the channels induced by threading dislocations so as to lead to variation of the forward voltage of blue LED during aging time. The breakage of current spreading layer induced the increase of the resistivity of the contact and semiconductor material and the degradation of the properties of the ohmic contacts, which correspond to increase of series resistance. So forward voltage variation for InGaN/GaN blue LED is highly related to the effect of changes in the series resistance.

The common electrical model for LED is composed of a ideal diode and series resistance. The voltage V_D across the ideal diode can be expressed in terms of the total voltage drop V across the series combination of the ideal diode and the series resistance. Thus, $V_D = V - IR$, and its current-

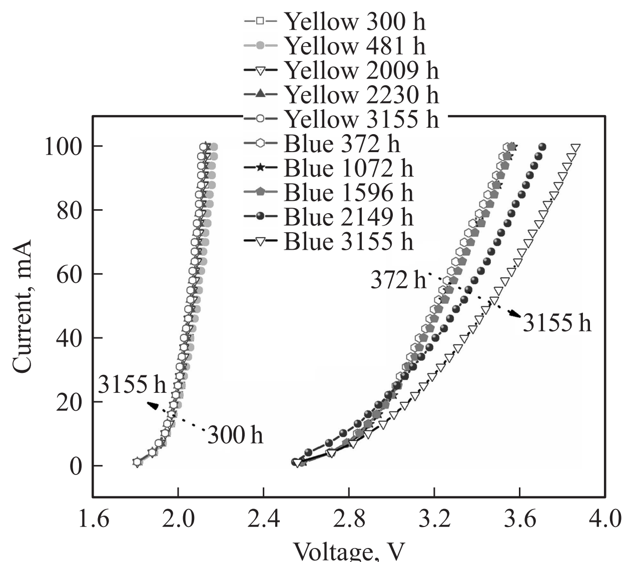

Figure 2. Forward $I-V$ characteristic of yellow and blue LED at 20 mA during aging process.

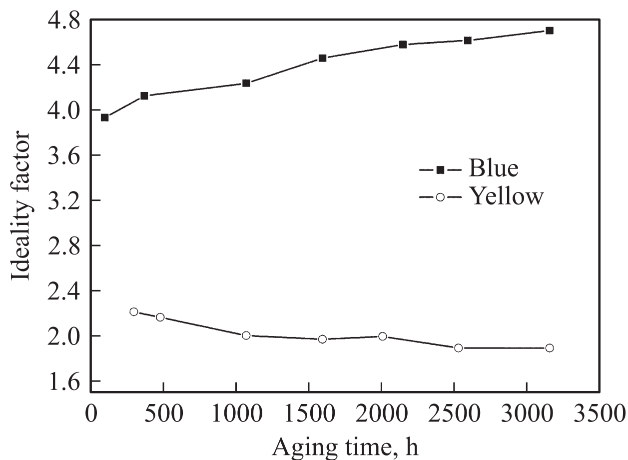

Figure 3. Ideality factor of yellow and blue LED at 20 mA during aging process.

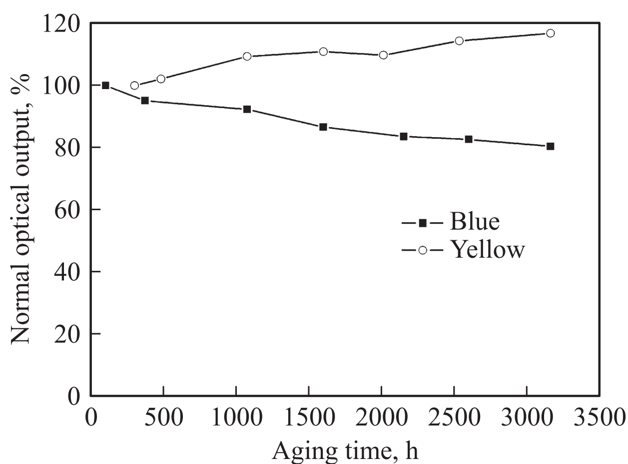

Figure 4. Normalized optical output of yellow and blue LED at 20 mA during aging process.

voltage($I-V$) characteristic is given by [16]

$$I = I_S \exp[q(V - IR)/nkT], \tag{4}$$

where I_S is the reverse saturation current, q is the electronic charge, k is the Boltzmann constant, T is the absolute temperature, and n is the ideality factor.

The ideality factor of blue LED is more than 2. The reason for the high ideality factor is attributed to tunneling and the influence of rectifying heterojunctions and metal–semiconductor junctions present heterostructure diodes [17,18]. The radiative recombination mechanism in LED with quantum well system in the depletion layer could be expected to give rise to the ideality factor [19]. The ideality factor of yellow LED is close to 2, indicating the recombination current is the major mechanism of the current transport, in contrast to that of blue LED. The ideality factor can be extracted from the $I-V$ characteristics by Eq. (1). Figs 3 and 4 show that ideality factors and optical output of blue and yellow LEDs during the aging period at 20 mA. It is noted that optical output of blue LEDs decrease as the increasing of aging time and optical output of yellow LEDs shows expansion behaviour with aging time. It can be assumed that optical output is linear with radiative recombination [20]. Based on the trend of ideality factors and optical output, the correlation between ideality factor and radiative recombination is roughly founded. The ideality factor of blue LED increases as aging time increase, which is attributed to the decrease of radiative recombination. On the contrary, since the radiative recombination of yellow LED faintly increase, the ideality factor decreases as a whole during aging period. Hence, the relationship of ideality factor and stress time can be used as prediction of the optical output degradation during aging process.

As shown in Fig. 5, under high level electrical stress, the degradation of optical output of InGaN/GaN blue LEDs is faster than that of AlGaInP yellow LED, which indicates that the defects highly affect the properties of blue LED more than yellow LED. The main cause of degradation in the inner region is directionally dependent on the crystal material. AlGaInP shows a much lower rate of dislocation growth than InGaN/GaN. Point defects can also lead to either slow or rapid degradation when the defects leads to plane defect in the crystal. Another fact is that the amount of photodegradation depends on the radiant intensity, emitting wavelength and time of exposure. Photodegradation is degradation of a photodegradable molecule caused by the absorption of photons, the process of decomposition of the material upon exposure to radiant energy such as the action of light. Most epoxy resin tends to absorb high-energy radiation of the spectrum, which activates their electrons to higher reactivity and causes oxidation, cleavage and other degradation. Photodegradation of epoxy resin will accelerated under the shorter emitting wavelength, high radiant intensity and long time of exposure. Therefore, even visible light of sufficient quantity can make polymer and epoxy materials degrade [21]. If the amounts of emitting photons are equal in different emitting wavelength, the

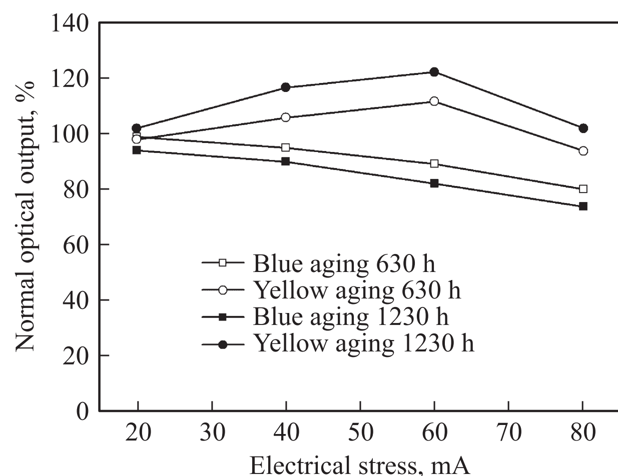

Figure 5. The normalized optical output of blue and yellow LED as a function of electrical stress at different aging time.

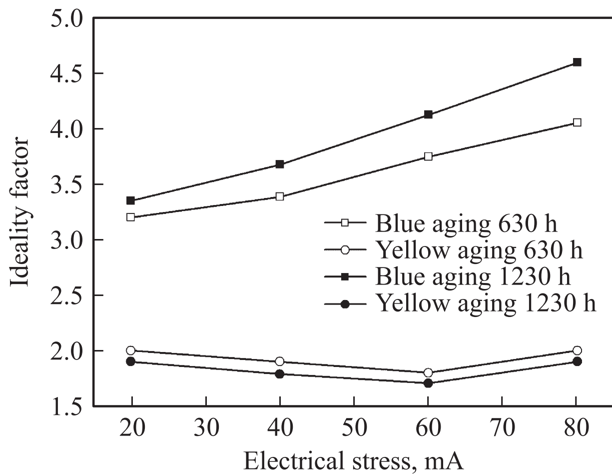

Figure 6. Electrical stress dependence of ideality factor at different aging time with yellow and blue LED.

shorter emitting wavelength of LED, the higher radiant energy excited, and the more photodegradation generation enhanced. That's why the blue LED has the higher rate of degradation than yellow LED.

After aging time of 1230 h, the optical output of blue LED decays drastically to 94.0, 89.8, 82.1 and 73.7% of initial optical output value, under three different electrical stresses of 20, 40, 60 and 80 mA, respectively. However, the yellow LED changes to 98.6, 105.2, 110.5 and 94.8% of initial optical output value under the same condition. When blue LED is stressed under different injection current, there are more carrier tunneling and the nonradiative recombination as generation point defects and line defects. The degradation mechanism of blue LED is due to the increase of nonradiative recombination centers defects in the active layers. Meanwhile, the efficiency losses also worsen the device performance.

The optical output of yellow LED almost keeps increasing behaviour as electrical stress, begin to decrease at 80 mA. Yellow LED can effectively control or eliminate nonradiative recombination centers in active regions during aging process. This „positive aging" mechanism explains that generation of nonradiative defect centers recombination channel is saturated [22].

From the experimental result, AlGaInP helps carriers eliminate the defects and increase tunneling current until large number of new point defects form. Compared to InGaN/GaN, AlGaInP has more radiative recombination carriers. Therefore, there is less chance of tunneling through active layers in AlGaInP.

$I-V$ characteristics of the AlGaInP yellow and InGaN/GaN blue LEDs were measured at 25°C. Fig. 6 shows the ideality factor of the yellow and blue LED as a function of electrical stress after 630 h aging. Combined

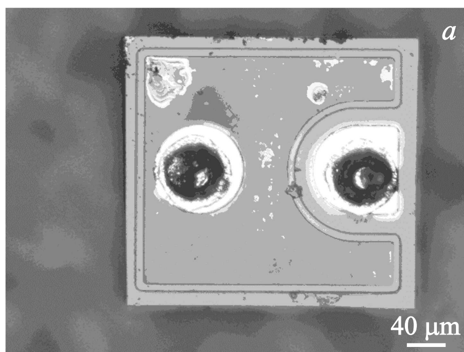

Blue LEG aging 1200 h at 20 mA

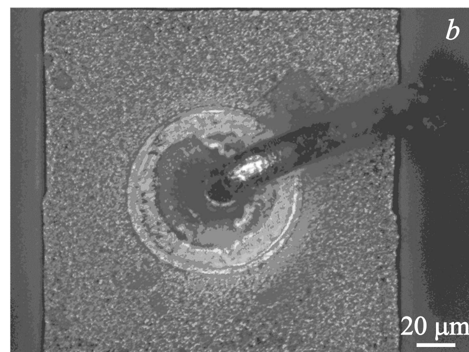

Yellow LED aging 1200 h at 20 mA

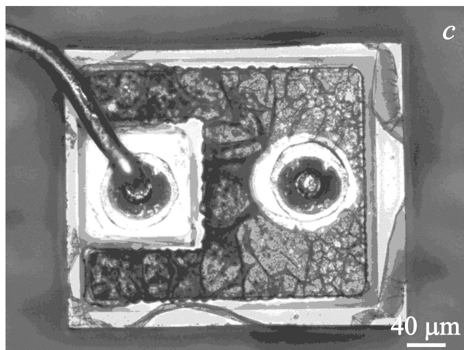

Blue LEG aging 2600 h at 80 mA

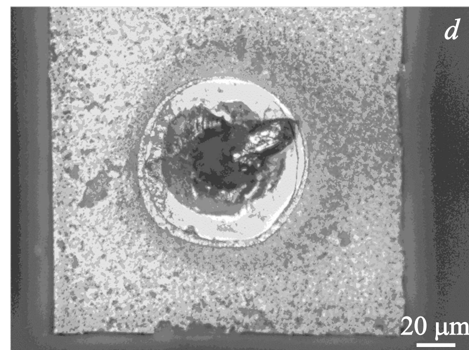

Yellow LED aging 2600 h at 80 mA

Figure 7. The photograph of blue and yellow LED under different electrical stress and aging time.

with Fig. 5, the ideality factor of blue LED increases as the increase of the degradation rate. Moreover, the yellow LED demonstrates a „positive aging“ at 20–60 mA with the reduction of ideality factor. It is indicated that the defects generated in the aging process reduce the optical output of blue LED more obviously. Since p-type transport properties generally get worsen due to the lower activation of acceptors at increasing electrical stress, the ideality factors of blue LED are 3.21, 3.39, 3.78 and 4.05 at 20, 40, 60 and 80 mA, respectively. It can use to predict the optical output degradation of LED based on the variation of the ideality factor during aging process. To investigate the electrical stress endurance of LED chips, Fig. 7 shows the photograph of LED chip for different electrical stress and aging time obtained by optical microscopes. As the current is injected into the LED during aging process, many dark spots and cracks can be observed on the blue LED at 80 mA, while the electrical stress of 20 mA shows better characteristic. With the breakage of current spreading layer, the light emission pattern of LED is less uniform so that the light output obviously decrease. On the other hand the yellow LED shows the integrality of current spreading layer and less of dark spots with the high electrical stress. Therefore the yellow LED is good reliable than blue LED during aging process.

The performance of intermediate adhesive layer, especially demonstrated by thermal properties, has obvious influence on the reliability of LED during aging process. The reliability of the intermediate adhesive layer depends on the individual chemistry parameters. The silver epoxy adhesive is applied between the reflector cup and AlGaInP LED chip with dimensions of $0.3 \times 0.3 \times 0.02$ mm. Fig. 8 illustrates the cumulative structure functions of the thermal resistance during aging process. By the cumulative structure functions, the thermal resistance between each layer of the LED package can be easily distinguished. As shown in Fig. 8, after 3155 h, the thermal resistance of the yellow LED chip has little change, but about 15.2 K/W increase is induced in the silver epoxy adhesive. Meanwhile, Fig. 9

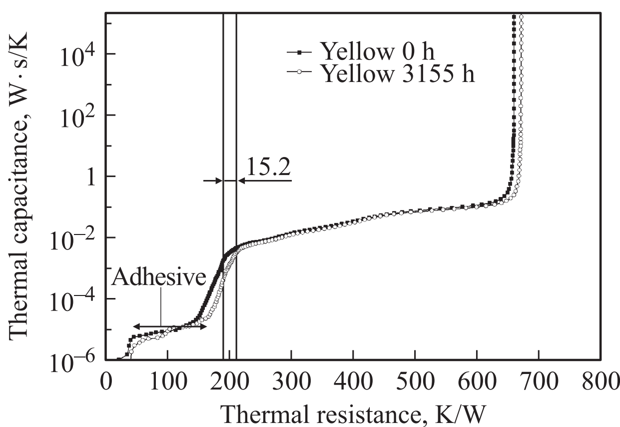

Figure 8. Cumulative structure functions of yellow LED during aging process.

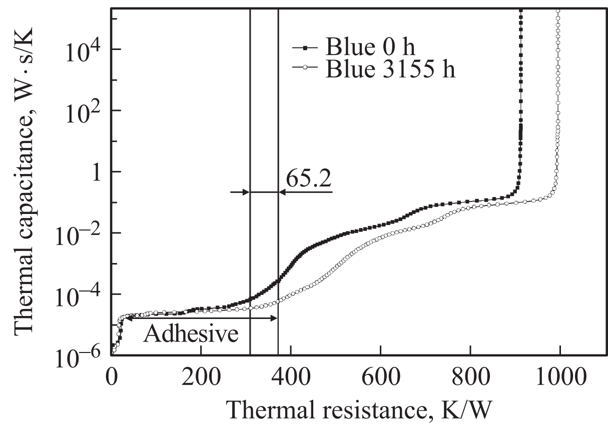

Figure 9. Cumulative structure functions of blue LED during aging process.

shows that under the same aging process, an increase of about 65.2 K/W in the insulative adhesive of blue LED appears. The heat generation inside the LED package can not be efficiently dissipated as the thermal resistance of intermediate adhesive layer increase, so the property of LED will be unstable. Hence, it offers further evidence for the faster optical output degradation of blue LED than that of yellow LED. Nickel-oxide formation on the surface of invar (Fe/Ni/Cu/Ag) submount is the factor for the increase of thermal resistance. Both oxidation and galvanic corrosion can cause the formation of metal oxide [23,24]. The delaminations of intermediate adhesive layer form during aging because of the large mismatch of coefficient of thermal expansions between the silver epoxy or insulative adhesive and invar(Fe/Ni/Cu/Ag) submount. On one hand, an interconnection gap can easily form around intermediate adhesive layer joints because metal does not expand as usual. On the other hand, the migration of conducting particles can induce the failure of intermediate adhesive layer joints during the current-induced resistance increase.

4. Conclusions

In summary, this paper investigated the electrical-thermal-optical aging properties of AlGaInP and InGaN/GaN LEDs under different electrical stresses. The forward voltages of AlGaInP LEDs decrease after 3155 h due to the increase in the effective acceptor concentration on p-type side. Based on the trend of ideality factors and optical output, the correlation between ideality factor and radiative recombination is founded. The result also indicates that the variation of ideality factor can be used as prediction of the optical output degradation during aging process. When the ideality factor of LED increases as aging time, the trend of ideality factor is attributed to generation of point defects that lead to more carriers tunneling in quantum wells as well as the nonradiative recombination. The change of the thermal resistance of the intermediate adhesive layer contributes

most during the aging process. After aging process, the heat generation inside the LED package can not be efficiently dissipated as the thermal resistance of intermediate adhesive layer increase, so the reliability of LED will be obviously unstable. Therefore, the main mechanism of degraded electrode is caused by metal diffusion into the inner region and is enhanced by junction temperature.

5. Acknowledgements

This work was supported by the Key Science Project of Fujian Province, China (Grant Nos. 2011H0021), 2011H6025, and 2012H0039), the Natural Science Foundation of Fujian Province, China (Grant No. 2011J05162), the Science Project of Education Bureau of Fujian Province, China (Grant No. JA11175) and the Foundation of Zhangzhou Normal University, China (Grant No. SJ1017).

References

[1] T. Egawa, T. Jimbo, M. Umeno. J. Appl. Phys., **82**, 5816 (1997).
[2] X.A. Cao, S.D. Arthur. Appl. Phys. Lett., **85**, 3971 (2004).
[3] T.J. Yu, S.P. Shang, Z.Z. Chen, Z.X. Qin, L. Lin, Z.J. Yang, GY. Zhang. J. Lumiescenc., **122**, 696 (2007).
[4] L. Sugiura. Appl. Phys. Lett., **70**, 1317 (1997).
[5] H.T. Chen, Y.J. Lu, Z. Chen, H.B. Zhang, L.Y. Gao, G.L. Chen. Acta Physica Sinca, **58**, 5688 (2009).
[6] F. Rossi, M. Pavesi, M. Meneghini, G. Salviati, M. Manfredi, G. Meneghesso, A. Castaldini, A. Cavallini, L. Rigutti, U. Strass, U. Zehnder, E. Zanoni. J. Appl. Phys., **99**, 053104-1 (2006).
[7] L.X. Zhao, E.J. Thrush, C.J. Humphreys, W.A. Phillips. J. Appl. Phys., **103**, 024501-1 (2008).
[8] A. Uddin, A.C. Wei, T.G. Andersson. Thin Sol. Films, **483**, 378 (2005).
[9] M. Meneghini, L. Trevisanello, C. Sanna, G. Mura, M. Vanzi, G. Meneghesso, E. Zanoni. Microelectron. Reliab., **47**, 1625 (2007).
[10] H.T. Chen, Y.J. Lu, Y.L. Gao, H.B. Zhang, Z. Chen. Thermochim. Acta, **488**, 33 (2009).
[11] V. Székely, T.V. Bien. Solid-State Electron., **31**, 1363 (1988).
[12] G. Farkas, Q.V. Vader. IEEE Trans. Compon. Pack. T, **28**, 45 (2005).
[13] M. Meneghini, L.R. Trevisanello, U. Zehnder, T. Zahner, U. Strauss, G. Meneghesso, E. Zanoni. IEEE Trans. Electron. Dev., **53** 2981 (2006).
[14] S.D. Lester, F.A. Ponce, M.G. Craford, D.A. Steigerwald. Appl. Phys. Lett., **66**, 1249 (1995).
[15] A. Usui, H. Sunakawa, A. Sakai, A.A. Yamaguchi. Jpn. J. Appl. Phys., **36**, 899 (1997).
[16] S.K. Cheung, N.W. Cheung. Appl. Phys. Lett., **49**, 85 (1986).
[17] X.A. Cao, J.M. Teetsov, M.P. D'Evelyn, D.W. Merfeld, C.H. Yan. Appl. Phys. Lett., **85**, 7 (2004).
[18] J.M. Shah, Y.L. Li, T. Gessmann, E.F. Schubert. J. Appl. Phys., **94** 2627 (2003).
[19] G. Franssen, E. Litwin-Staszewska, R. Piotrzkowski, T. Suski, P. Perlin. J. Appl. Phys., **94**, 6122 (2003).
[20] P.N. Grillot, M.R. Krames. IEEE Trans. Dev. Mat. Relinb., **6**, 564 (2006).
[21] A. Torikal, H. Hasegawa. Polym. Degrad. Stab., **63**, 441 (1999).
[22] O. Pursiainen, N. Linder, A. Jaeger, R. Oberschmid, K. Streubel. Appl. Phys. Lett., **79**, 2895 (2001).
[23] J. Liu, K. Boustedt, Z. Lai. Circuit World, **22** 19 (1996).
[24] H.K. Kim, F.G. Shi. Microelectronics J., **32**, 315 (2001).

Редактор Т.А. Полянская